THEORETICAL-EXPERIMENTAL ANALYSIS OF CONJUGATED CONDUCTION-CONVECTION IN MICRO-CHANNELS UNDER ASYMMETRIC CONDITIONS

Jeziel S. Nunes, jeziel@inpi.gov.br
INPI, Rio de Janeiro, Brasil
Mila R. Avelino, mila@uerj.br
Mechanical Eng. Dept. – UERJ, Rio de Janeiro, Brasil
Renato M. Cotta, cotta@mecanica.coppe.ufrj.br
Laboratory of Transmission and Technology of Heat, LTTC
Mechanical Engineering Dept. – POLI & COPPE/UFRJ
Universidade Federal do Rio de Janeiro, Cx. Postal 68503
Cidade Universitária – Rio de Janeiro, RJ – 21945-970 – Brasil

Abstract. *The present work theoretically and experimentally analyzes the conjugated heat transfer problem for laminar flow in micro-scale, with the simultaneous determination of the temperature fields in the liquid and solid regions of a rectangular micro-channel formed by parallel plates made of distinct materials and subjected to asymmetric thermal conditions. The methodology that has been applied in the modeling and solution of this problem consists in the application of the Lumped System Approach to the solid boundaries adjacent to fluid, and, subsequently, applying the Generalized Integral Transform Technique (GITT) to obtain an ordinary differential transformed system which is solved in the computational platform Mathematica 7.0. An experimental setup was designed and built for the determination of Nusselt numbers in a parallel plates channel made of tin and copper inside a PMMA – (poly-methyl methacrylate) prism, with Joule effect heating on the tin side. Experimental runs for different Reynolds numbers allowed for obtaining a significant set of experimental results for a micro-channel height of 270 microns, offering comparisons and validation of the model here proposed.*

Keywords*: Micro-channel, forced convection, conjugated problem, heat exchanger, Nusselt number*

1. INTRODUCTION

Energy conservation and sustainable development demands have been driving research efforts, within the scope of thermal engineering, towards more energy efficient equipments and processes. In this context, the scale reduction in mechanical fabrication has been permitting the miniaturization of thermal devices, such as in the case of micro-heat exchangers (Sobhan & Peterson, 2008). More recently, heat exchangers employing micro-channels with characteristic dimensions below 500 microns have been calling the attention of researchers and practitioners, towards applications that require high heat removal demands and/or space and weight limitations (Yener et al., 2005). Thus, micro-fabrication techniques have been allowing for the improvement and development of a number of engineering applications, while providing new challenging scientific perspectives in fundamental research.

Recent review works (Morini, 2004; Yener et al., 2005) have pointed out discrepancies between experimental results and classical correlation predictions of heat transfer coefficients in micro-channels. Such deviations have been stimulating theoretical research efforts towards a better agreement between experiments and simulations, through the incorporation of different effects that are either typically present in micro-scale heat transfer or are effects that are normally disregarded at the macro-scale and might have been erroneously not accounted for in micro-channels. Our own research effort was first related to the fundamental analysis of forced convection within micro-channels with and without slip flow, as required for the design of micro-heat exchangers in steady, periodic and transient regimen (Mikhailov & Cotta, 2005; Cotta et al., 2005; Castellões & Cotta, 2006; Castellões et al., 2007). Then, this fundamental research was extended to include the effects of axial fluid heat conduction and wall corrugation or roughness on heat transfer enhancement (Castellões & Cotta, 2008). The research on heat transfer enhancement at the micro-scale also progressed to the experimental investigation of rough micro-tubes and to the study of conjugated effects in rectangular micro-channels (Nunes et al., 2008). Interesting examples that further motivated the present analysis are the works of Castilho (2003) and Maranzana et al. (2004) dealing with longitudinal wall heat conduction effects in symmetric micro-channels. Conjugated conduction-convection problems are among the classical formulations in heat transfer that still demand exact analytical treatment. Since the pioneering works of Perelman (1961) and Luikov et al. (1971), such class of problems continuously deserved the attention of various researchers towards the development of approximate formulations and/or solutions, either in external or internal flow situations. For instance, the present integral transform approach itself has been applied to obtain hybrid solutions for conjugated conduction-convection problems (Guedes et al., 1991; Guedes & Cotta, 1992; Naveira et al., 2009), in both steady and transient formulations, by employing a transversally lumped heat conduction equation for the wall temperature.

The present work then illustrates theoretical-experimental research efforts on forced convection in micro-channels, trying to focus on the fundamental aspects that are required to play some role in matching the classical heat transfer models to available or produced experimental results in laminar forced convection. The first aim was to address the walls conjugation effects for a parallel-plates micro-channel, micro-machined from metallic plates, subjected to asymmetric thermal boundary conditions. The typical low Reynolds numbers in such micro-systems may lead to low values of the Peclet number that bring up some relevance to the axial heat diffusion along the fluid stream, especially for regions close to the inlet. Thus, both the bounding walls and the fluid axial diffusion may participate in the overall heat transfer process, and yield different predictions than those reached by making use of conventional macro-scale relations for ordinary liquids.

All the theoretical work was performed by making use of mixed symbolic-numerical computation via the *Mathematica 7.0* platform (Wolfram, 2008), and a hybrid numerical-analytical methodology with automatic error control, the Generalized Integral Transform Technique – GITT (Cotta, 1993; Cotta & Mikhailov, 1997; Cotta, 1998; Cotta & Mikhailov, 2006), in handling the governing partial differential equations. Experimental results are then briefly discussed and presented to verify the proposed models.

2. PROBLEM FORMULATION AND SOLUTION METHODOLOGY

The objective of this research was to theoretically and experimentally analyze the conjugated heat transfer problem in micro-scale for laminar flow, involving the simultaneous determination of the temperature fields in the liquid and solid regions of a rectangular micro-channel formed by parallel plates made of distinct materials and subjected to asymmetric thermal conditions. The methodology that has been applied in the modeling and solution of this problem consists in the application of the Lumped System Approach to the solid boundaries adjacent to fluid, which are then transformed into boundary conditions for the convection problem and, subsequently, applying the Generalized Integral Transform Technique (GITT) to obtain an ordinary differential transformed system solved by an adequate routine in the *Mathematica* computational platform. An experimental setup was designed and built for the determination of Nusselt numbers in a parallel plate channel made of tin and copper, with Joule effect heating on one side and adjustable distance between the plates. Experimental runs for different Reynolds numbers allowed for obtaining a significant set of experimental results for a micro-channel height of 270μm, offering comparisons and validation of the proposed model.

We consider thermally developing forced convection of a Newtonian fluid in the continuum regimen, under fully developed laminar flow inside a rectangular micro-channel formed by parallel layers of different materials and/or thicknesses, and subjected to an inlet temperature T_e. The walls are assumed to participate in the heat transfer process within the fluid along the channel length, and to exchange heat with the external environment with the temperature T_{ext} and a heat transfer coefficient h_{ext}, according to Figure 1 below. In addition, the walls are allowed to uniformly generate heat.

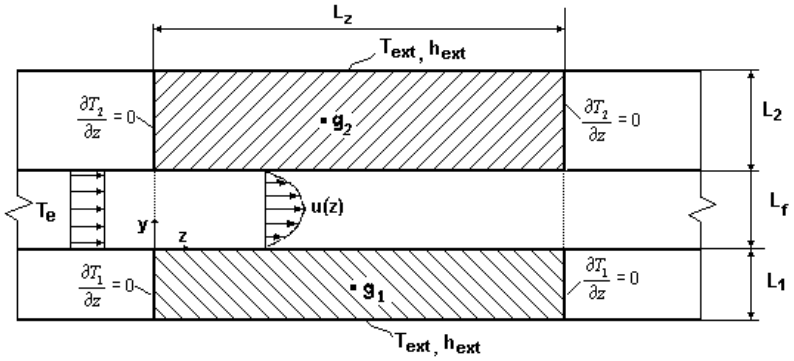

Figure 1. Geometry and coordinates system for asymmetric conjugated heat transfer in micro-channels.

The thermophysical properties of all the materials are taken as constant and the conjugated problem can be written in dimensionless form as follows:

$$\frac{\partial^2\theta_1}{\partial\eta^2}+\frac{1}{(2Pe)^2}\frac{\partial^2\theta_1}{\partial\zeta^2}+Q_1=0; \qquad -l_{\eta 1}<\eta<0; \quad 0<\zeta<l_\zeta \tag{1a}$$

$$\frac{U(\eta)}{4}\frac{\partial\theta_f}{\partial\zeta}=\frac{\partial^2\theta_f}{\partial\eta^2}+\frac{1}{(2\mathrm{Pe})^2}\frac{\partial^2\theta_f}{\partial\zeta^2}+\mathrm{Br}\left(\frac{\mathrm{dU}(\eta)}{d\eta}\right)^2 \qquad 0<\eta<1 \qquad \zeta>0 \tag{1b}$$

$$\frac{\partial^2\theta_2}{\partial\eta^2}+\frac{1}{(2Pe)^2}\frac{\partial^2\theta_2}{\partial\zeta^2}+Q_2=0; \qquad 1<\eta<l_{\eta 2} \quad 0<\zeta<l_\zeta \tag{1c}$$

where the three energy equations above refer, respectively, to the lower wall, to the fluid and to the upper wall in Figure 1. The following boundary and inlet conditions are proposed:

$$\frac{\partial \theta_1}{\partial \zeta}=0 \qquad \zeta = 0, \qquad \frac{\partial \theta_1}{\partial \zeta}=0 \qquad \zeta = l_\xi \tag{2a,b}$$

$$\frac{\partial \theta_2}{\partial \zeta}=0 \qquad \zeta = 0, \qquad \frac{\partial \theta_2}{\partial \zeta}=0 \qquad \zeta = l_\zeta \tag{2c,d}$$

$$-\frac{\partial \theta_1}{\partial \eta}+Bi_{\eta 1}\theta_1=0 \qquad \eta = -l_{\eta 1}, \qquad \frac{\partial \theta_2}{\partial \eta}+Bi_{\eta 2}\theta_2=0 \qquad \eta = l_{\eta 2} \tag{2e,f}$$

$$\theta_f(\eta,\zeta)=1 \quad \zeta = 0, \qquad \frac{\partial \theta_f}{\partial \zeta}=0 \qquad \zeta = l_\zeta \tag{2g,h}$$

besides the interface conditions

$$\theta_f = \theta_1 \quad \eta = 0, \qquad k_1^* \frac{\partial \theta_f}{\partial \eta} = \frac{\partial \theta_1}{\partial \eta} \qquad \eta = 0 \tag{2i,j}$$

$$\theta_f = \theta_2 \quad \eta = 1 \qquad 0 < \zeta < l_\zeta, \qquad k_2^* \frac{\partial \theta_f}{\partial \eta} = \frac{\partial \theta_2}{\partial \eta} \qquad \eta = 1 \qquad 0 < \zeta < l_\zeta \tag{2k,l}$$

The following dimensionless relations were here employed:

$$\theta_i = \frac{T_i - T_\infty}{T_0 - T_\infty}, \text{ where } i = 1,\ 2,\ f\ ; \qquad \zeta = \frac{z}{\mathrm{Pr}\,\mathrm{Re}\,D_h}; \qquad \eta = \frac{y}{L_f};$$

$$D_h = \frac{4S}{P} \Rightarrow \frac{4(L_f * L_w)}{2(L_f + L_w)}, \text{ since } L_w >> L_f \Rightarrow D_h = 2L_f;$$

$$U(\eta) = \frac{u(y)}{\bar{u}}; \qquad \frac{\mathrm{d}\zeta}{\mathrm{dz}} = \frac{1}{\mathrm{Pr}\,\mathrm{Re}\,Dh}; \qquad \frac{d\eta}{dy} = \frac{1}{L_f}; \tag{3a-k}$$

$$\mathrm{Pe} = \mathrm{Re}\,\mathrm{Pr}; \qquad \mathrm{Re} = \frac{\bar{u} D_h}{\nu}; \quad \mathrm{u(y)} = 3y(1-2y)$$

and,

$$Q_1 = \frac{\mathrm{g}_1 L_f^2}{\mathrm{k}_1 \Delta T},\ W(\eta) = \frac{U(\eta)}{4}, \quad Q_2 = \frac{\mathrm{g}_2 L_f^2}{\mathrm{k}_2 \Delta T} \quad \text{and} \quad Br = \frac{\mu}{k}\frac{u}{\Delta T} \tag{3l-o}$$

$$k_1^* = \frac{k_f}{k_1}; \quad k_2^* = \frac{k_f}{k_2}; \quad l_{\eta 1} = \frac{L_1}{L_f}, \quad l_{\eta 2} = \frac{L_2 + L_f}{L_f} \tag{3p-s}$$

where the indexes *1* and *2* denote the lower and upper solid layers, and f refers to the fluid.

The Classic Lumped System Analysis is applied to the energy equations of the two solid layers that define the walls of the channel. This reformulation and simplification strategy is feasible once the temperature gradients across both walls are sufficiently smooth, a behavior governed by the magnitudes of the Biot numbers at each face of the two walls. For instance, considering the thermally thin-walled hypothesis for layer 1 above, the lumping procedure assumes that

$$\theta_1(-l_{\eta 1}, \zeta) \cong \theta_1(0, \zeta) \cong \theta_{av,1}(\zeta) \tag{4a}$$

where $\theta_{av,1}(\zeta)$ is calculated by the transversally averaged temperature definition:

$$\theta_{av,1}(\zeta) = \frac{1}{l_{\eta 1}} \int_{-l_{\eta 1}}^{0} \theta_1(\eta, \zeta)\, d\eta \tag{4b}$$

Equation (1a) for $\theta_1(\eta,\zeta)$ is thus integrated in the η direction, applying the integral operator $\frac{1}{l_{\eta 1}}\int_{-l_{\eta 1}}^{0} \_\_ d\eta$ in both the energy equation and required boundary conditions, providing after some manipulation:

$$-\frac{\partial \theta_f}{\partial \eta} + Bi_{\eta 1}^* \theta_f = \frac{l_{\eta 1}}{(2Pe)^2} \left.\frac{\partial^2 \theta_f(\eta,\zeta)}{\partial \zeta^2}\right|_{\eta=0} + Q_1^* \qquad \eta = 0 \tag{5a}$$

where

$$Bi_{\eta 1}^* = \frac{Bi_{\eta 1}}{k_1^*} \quad \text{and} \quad Q_1^* = \frac{l_{\eta 1}}{k_1^*} \mathrm{Q}_1 \tag{5b,c}$$

The same procedure is then applied to layer 2, Eq.(1c), which results in:

$$\frac{\partial \theta_f}{\partial \eta} + Bi_{\eta 2}^* \theta_f = \frac{(l_{\eta 2} - 1)}{k_2^* (2Pe)^2} \left.\frac{\partial^2 \theta_f(\eta,\zeta)}{\partial \zeta^2}\right|_{\eta=1} + Q_2^* \qquad \eta = 1 \tag{5d}$$

where

$$Bi^*_{\eta 2} = \frac{Bi_{\eta 2}}{k_2^*} \quad \text{and} \quad Q_2^* = \frac{\left(l_{\eta 2} - 1\right)}{k_2^*} \mathrm{Q}_2 \tag{5e,f}$$

Thus, application of the lumping procedure to the original formulation leads to the extended Graetz problem described by the equation and boundary conditions below:

$$W(\eta)\frac{\partial \theta_f}{\partial \zeta} = \frac{\partial^2 \theta_f}{\partial \eta^2} + \frac{1}{(2Pe)^2}\frac{\partial^2 \theta_f}{\partial \zeta^2} + Br\left(\frac{dU(\eta)}{d\eta}\right)^2, \quad 0<\eta<1, \quad \zeta>0 \tag{6a}$$

$$-\frac{\partial \theta_f}{\partial \eta} + Bi^*_{\eta 1}\theta_f = Cj_1 \frac{\partial^2 \theta_f(\eta,\zeta)}{\partial \zeta^2} + Q_1^*, \qquad \eta = 0 \tag{6b}$$

$$\frac{\partial \theta_f}{\partial \eta} + Bi^*_{\eta 2}\theta_f = Cj_2 \frac{\partial^2 \theta_f(\eta,\zeta)}{\partial \zeta^2} + Q_2^*, \qquad \eta = 1 \tag{6c}$$

$$\theta_f(\eta,\zeta) = 1 \qquad \zeta = 0, \qquad \frac{\partial \theta_f}{\partial \eta} = 0 \qquad \zeta = l_\zeta \tag{6d,e}$$

where Cj_1 and Cj_2 are the conjugation coefficients, respectively, in the lower and upper walls, as:

$$Cj_1 = \frac{l_{\eta 1}}{(2Pe)^2 k_1^*}; \quad Cj_2 = \frac{l_{\eta 2} - 1}{(2Pe)^2 k_2^*} \tag{6f,g}$$

Eqs. (6) are now solved by the Generalized Integral Transform Technique, GITT, starting with the choice of an appropriate filtering solution that eliminates the non-homogeneous terms in the equation and boundary conditions:

$$\theta_f(\eta,\zeta) = \theta_H(\eta,\zeta) + \theta_P(\eta) \tag{7}$$

A fairly simple filter in terms of a purely diffusive formulation in the transversal direction is proposed:

$$\frac{d^2\theta_P(\eta)}{d\eta^2} + Br\left(\frac{d(U(\eta)}{d\eta}\right)^2 = 0 \qquad 0<\eta<1 \qquad \zeta>0 \tag{8a}$$

$$-\frac{d\theta_P(\eta)}{d\eta} + Bi^*_{\eta 1}\theta_P(\eta) = Q_1^* \qquad \eta = 0$$
$$\frac{d\theta_P(\eta)}{d\eta} + Bi^*_{\eta 2}\theta_P(\eta) = Q_2^* \qquad \eta = 1 \tag{8b,c}$$

The filtered problem formulation is then given by:

$$W(\eta)\frac{\partial \theta_H(\eta,\zeta)}{\partial \zeta} - \frac{1}{(2Pe)^2}\frac{\partial^2 \theta_H(\eta,\zeta)}{\partial \zeta^2} = \frac{\partial^2 \theta_H(\eta,\zeta)}{\partial \eta^2} \qquad 0<\eta<1 \qquad \zeta>0 \tag{9a}$$

$$\theta_H(\eta,\zeta) = 1 - \theta_P(\eta), \quad \zeta = 0; \qquad \frac{\partial \theta_H(\eta,\zeta)}{\partial \eta} = 0, \quad \zeta = l_\zeta \tag{9b,c}$$

$$-\frac{\partial \theta_H(\eta,\zeta)}{\partial \eta} + Bi^*_{\eta 1}\theta_H(\eta,\zeta) = Cj_1 \frac{\partial^2 \theta_H(\eta,\zeta)}{\partial \zeta^2} \qquad \eta = 0$$
$$\frac{\partial \theta_H(\eta,\zeta)}{\partial \eta} + Bi^*_{\eta 2}\theta_H(\eta,\zeta) = Cj_2 \frac{\partial^2 \theta_H(\eta,\zeta)}{\partial \zeta^2} \qquad \eta = 1 \tag{9d,e}$$

The auxiliary problem that forms the basis for the eigenfunction expansion is then proposed:

$$\frac{d^2\psi_i(\eta)}{d\eta^2} + \beta_i^2 W(\eta)\psi_i(\eta) = 0, \qquad 0<\eta<1 \tag{10a}$$

$$-\frac{d\psi_i(\eta)}{\partial \eta} + Bi^*_{\eta 1}\psi_i(\eta) = 0, \quad \eta = 0; \quad \frac{d\psi_i(\eta)}{\partial \eta} + Bi^*_{\eta 2}\psi_i(\eta) = 0, \quad \eta = 1 \tag{10b,c}$$

Then, the integral transform pair is constructed for application of the GITT:

$$\begin{cases} \overline{\theta}_i(\zeta) = \int_0^1 W(\eta)\psi_i(\eta)\theta_H(\eta,\zeta)\,d\eta & \text{transform} \\ \theta_H(\eta,\zeta) = \sum_{i=1}^{\infty} \frac{\psi_i(\eta)}{N_i}\overline{\theta}_i(\zeta) & \text{inverse} \end{cases} \tag{11a,b}$$

where the norm is given by:

$$N_i = \int_0^1 W(\eta)\psi_i(\eta)^2\,d\eta \tag{11c}$$

Using the integral operator in Eq. (11a) and applying the 2nd Green´s formula, the transformed system is obtained as:

$$\frac{d\bar{\theta}_i(\zeta)}{d\zeta}+\beta_i^2\bar{\theta}_i(\zeta)=Cj_1\psi_i(0)\left.\frac{\partial^2\theta_H}{\partial\zeta^2}\right|_{\eta=0}+Cj_2\psi_i(1)\left.\frac{\partial^2\theta_H}{\partial\zeta^2}\right|_{\eta=1}+\frac{1}{(2Pe)^2}\int_0^1\psi_i(\eta)\frac{\partial^2\theta_H}{\partial\zeta^2}d\eta \quad \zeta>0 \tag{12a}$$

Employing the inverse formula in the axial diffusion term, $\frac{1}{(2Pe)^2}\int_0^1\psi_i(\eta)\frac{\partial^2\theta_H}{\partial\zeta^2}d\eta$, we find:

$$\sum_{j=1}^{\infty}\frac{1}{(2Pe)^2}\frac{d^2\bar{\theta}_j(\zeta)}{d\zeta^2}\frac{1}{N_j}\underbrace{\int_0^1\psi_i(\eta)\psi_j(\eta)d\eta}_{I\psi_{ij}}=\sum_{j=1}^{\infty}\frac{1}{(2Pe)^2}\frac{d^2\bar{\theta}_j(\zeta)}{d\zeta^2}\frac{I\psi_{ij}}{N_j} \tag{12b}$$

Replacing directly into Eq.(12a) the relations found in the modified boundary conditions, Eqs. (9d,e), we have:

$$\begin{aligned}\frac{d\bar{\theta}_i(\zeta)}{d\zeta}+\beta_i^2\bar{\theta}_i(\zeta)=\psi_i(0)\left(-\left.\frac{\partial\theta_H}{\partial\eta}\right|_{\eta=0}+Bi^*_{\eta1}\theta_{w1}(\zeta)\right)+\psi_i(1)\left(\left.\frac{\partial\theta_H}{\partial\eta}\right|_{\eta=1}+Bi^*_{\eta2}\theta_{w2}(\zeta)\right)+\\ +\sum_{j=1}^{\infty}\frac{1}{(2Pe)^2}\frac{d^2\bar{\theta}_j(\zeta)}{d\zeta^2}\frac{I\psi_{ij}}{N_j}\quad 0<\eta<1\quad \zeta>0\end{aligned} \tag{12c}$$

where $\theta_{w1}(\zeta)=\theta_f(0,\zeta)$ and $\theta_{w2}(\zeta)=\theta_f(1,\zeta)$.

After substitution of the inverse formulae in the remaining terms, and some rearrangement, the transformed ODE system is written as:

$$\begin{aligned}\sum_{j=1}^{\infty}aa_{ij}\frac{d^2\bar{\theta}_j(\zeta)}{d\zeta^2}-\sum_{j=1}^{\infty}\delta_{ij}\frac{d\bar{\theta}_j(\zeta)}{d\zeta}-\sum_{j=1}^{\infty}a_{ij}\bar{\theta}_j(\zeta)=\\ -\left[g_{1i}\theta_{w1}(\zeta)+g_{2i}\theta_{w2}(\zeta)_i\right]\quad 0<\eta<1\quad \zeta>0\end{aligned} \tag{13a}$$

where

$$\mathbf{A}=\{a_{ij}\}\begin{cases}\beta_i^2-\frac{1}{N_j}\left(\psi_i(1)\left.\frac{d\psi_i}{d\eta}\right|_{\eta=1}-\psi_i(0)\left.\frac{d\psi_i}{d\eta}\right|_{\eta=0}\right) & i\le N\quad j\le N\quad i=j\\ -\frac{1}{N_j}\left(\psi_i(1)\left.\frac{d\psi_j}{d\eta}\right|_{\eta=1}-\psi_i(0)\left.\frac{d\psi_j}{d\eta}\right|_{\eta=0}\right) & i\le N\quad j\le N\quad i\ne j\end{cases} \tag{13b,c}$$

$$[AA]=\{aa_{ij}\}=\frac{1}{(2Pe)^2}\frac{I\psi_{ij}}{N_j}\qquad \forall i,j\begin{cases}i\le N\\ j\le N\end{cases} \tag{13d}$$

$$g_1=\{Bi^*_{\eta1}\psi_i(0)\},\quad g_2=\{Bi^*_{\eta2}\psi_i(1)\},\qquad i\le N \tag{13e,f}$$

The equations that govern the wall temperatures are then rewritten as:

$$\begin{aligned}\frac{d\theta'_{w1}}{d\zeta}=-\frac{1}{Cj_1}\sum_{j=1}^{N}\frac{1}{N_j}\left.\frac{\partial\psi_j}{\partial\eta}\right|_{\eta=0}\bar{\theta}_j(\zeta)+\frac{Bi^*_{\eta1}}{Cj_1}\theta_{w1}(\zeta)\\ \frac{d\theta'_{w2}}{d\zeta}=\frac{1}{Cj_2}\sum_{j=1}^{N}\frac{1}{N_j}\left.\frac{\partial\psi_j}{\partial\eta}\right|_{\eta=1}\bar{\theta}_j(\zeta)+\frac{Bi^*_{\eta2}}{Cj_2}\theta_{w2}(\zeta)\end{aligned} \tag{14a,b}$$

The boundary conditions for the transformed temperatures and wall temperatures are given by:

$$\bar{\theta}_i(\zeta)=\bar{f}_i\qquad \zeta=0,\quad \bar{\theta}'_i(\zeta)=0\qquad \zeta=l_\zeta,\quad i=1,2,...,N \tag{14c,d}$$

$$\left.\frac{d\theta_{w1}}{d\zeta}\right|_{\zeta=0}=0;\quad \left.\frac{d\theta_{w1}}{d\zeta}\right|_{\zeta=l_\zeta}=0;\quad \left.\frac{d\theta_{w2}}{d\zeta}\right|_{\zeta=0}=0;\quad \left.\frac{d\theta_{w2}}{d\zeta}\right|_{\zeta=l_\zeta}=0 \tag{14e-h}$$

where

$$\bar{f}_i=\int_0^1 W(\eta)\psi_i(\eta)(1-\theta_P(\eta))d\eta \tag{14i}$$

Due to the slower convergence rates expected from the above formal solution once the inverse formula is substituted back into Eq. (12c), as noted in Guedes et al. (1991), the energy equation is integrated across the transversal domain, as described in Cotta (1993) and named as the integral balance scheme, in order to reach an improved convergence behavior in the representation of the derivatives and temperatures at the boundary positions. Thus, the fluid energy equation is integrated across the channel, and the inverse formula is substituted for the bulk temperature within the convection term, providing alternative expressions for the boundary derivatives. This procedure can be found in detail in Nunes et al. (2008).

Thus, the following ODE system truncated to order N is to be solved:

$$\{Y'(\zeta)\} = [C]\{Y(\zeta)\}, \tag{15a}$$

$$Y(\zeta) = \left\{\bar{\theta}_1(\zeta), \bar{\theta}_2(\zeta), \bar{\theta}_3(\zeta), ..., \bar{\theta}_N(\zeta), \bar{\theta}_1'(\zeta), \bar{\theta}_2'(\zeta), \bar{\theta}_3'(\zeta), ..., \bar{\theta}_N'(\zeta), \bar{\theta}_{w1}(\zeta), \bar{\theta}_{w2}(\zeta), \bar{\theta}_{w1}'(\zeta), \bar{\theta}_{w2}'(\zeta)\right\}^T \tag{15b}$$

which requires the computation of the eigenvalues and eigenvectors of matrix **C** to yield the solution vector Y, or:

$$(C - I\lambda)\xi = 0, \qquad Y(\zeta) = \sum_{k=1}^{N+4} c_k \xi_k e^{\lambda_k \zeta} \tag{15c,d}$$

It should be noticed that the averaged wall temperatures, $\theta_{w1}(\zeta)$ and $\theta_{w2}(\zeta)$, are directly obtained from the solution vector $Y(\zeta)$ as positions N+1 and N+2, as well as their longitudinal derivatives (positions N+3 and N+4).

The fluid bulk temperature is given by the working expression below:

$$\theta_{av}(\zeta) = \frac{\sum_{i=1}^{N} \int_0^1 W(\eta)\psi_i(\eta)d\eta \dfrac{\bar{\theta}_i(\zeta)}{N_i}}{\int_0^1 W(\eta)d\eta} + \frac{\int_0^1 W(\eta)\theta_P(\eta)d\eta}{\int_0^1 W(\eta)d\eta} \tag{16}$$

For the computation of the associated local Nusselt numbers, the derivatives at the walls of the fluid temperature are obtained by making use of the expressions previously derived with the integral balance scheme, or simply in the more direct form illustrated below for wall 1:

$$Nu_1 = \frac{-2\left(\sum_{i=1}^{\infty} \left.\dfrac{d\psi_i(\eta)}{d\eta}\right|_{\eta=0} \dfrac{\bar{\theta}_i(\zeta)}{N_i} + \left.\dfrac{d\theta_p(\eta)}{d\eta}\right|_{\eta=0}\right)}{\theta_{w1}(\zeta) - \theta_{av}(\zeta)} \tag{17}$$

3. EXPERIMENTAL APPARATUS AND PROCEDURE

Before obtaining the experimental results for the proposed covalidation effort, two prior steps were required, namely, the design and fabrication of the microchannels, and the assembly of an experimental platform that would allow for the easy exchange of different microchannel setups. A PMMA – *(poly-methyl methacrylate)* prism of low thermal conductivity was employed as the structural support of the metallic plates that form the microchannels, chosen to be made of electronic grade copper (upper plate) and tin (lower plate). Micro-machining of the PMMA block and of the metallic plates was accomplished and the setup was assembled according to Figures 2 below.

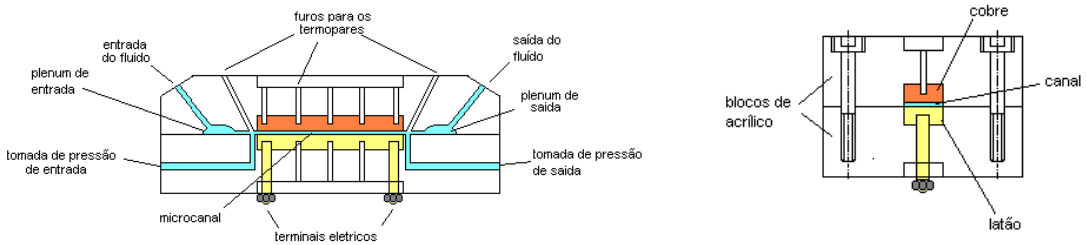

Figure 2.a) Schematic representation of the microchannel assembly; b)Cross section view of the assembly

Figures 3 show the assembled microchannel setup, within the PMMA block, and the installed thermocouples at both the lower (Fig.3.a) and the upper (Fig.3.b) plates. The employed technique allowed for the fabrication of microchannels up to 20 μm of plates spacing and uncertainty of $\pm$ 2.0μm.

Figure 3 – Details of the lower and upper plates of the microchannel setup with installed thermocouples.

The complete experimental platform is shown in Figure 4 below, which is fully automated, both in the data acquisition and on the control of the flow and heating parameters. The concept was that of allowing for straightforward interchanges of the microchannel setups without modifications of the remaining of the platform.

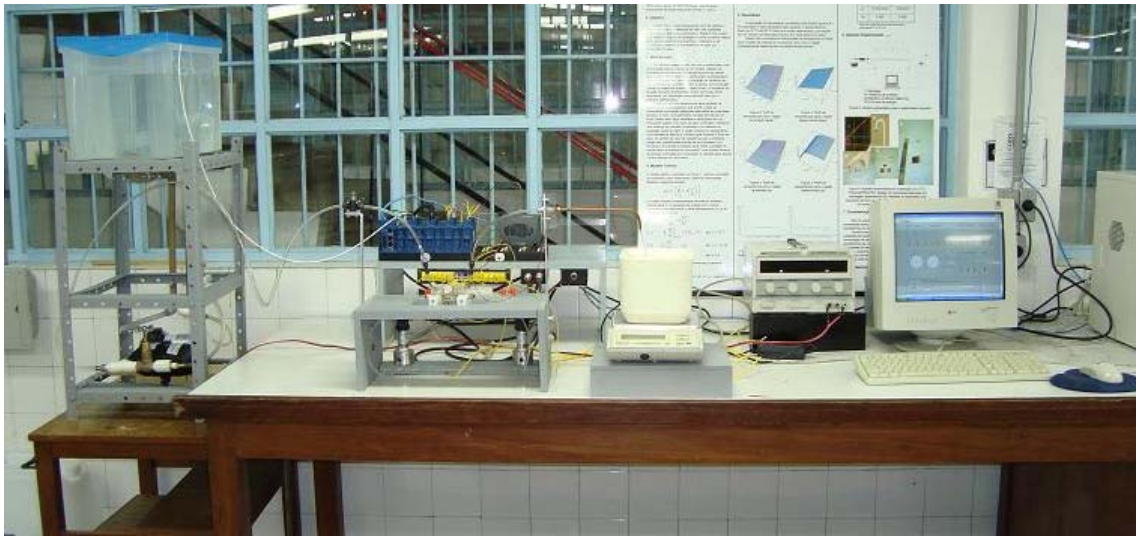

Figure 4 – General view of the experimental platform.

The microchannel wall was heated by Joule effect through an alternate current circuit of 220 V and 33 A. Temperature measurements were taken with type E (chromel-constantan) and type K (chromel-alumel) thermocouples, with uncertainty to within 0.3ºC. Pressure difference measurements were obtained with membrane type pressure tranduscers, model S10 from WIKA Alexander Wiegand GmbH & C.KG, 0-10 bar (4 to 20 mA). Mass flow rate was determined with the aid of an electronic scale MARTE model AS 2200 (0-2000g, $\pm$ 0.0001g). The acquisition system was based on a microcomputer Pentium IV with 2Gb of RAM, HD of 80Mb, and RS 232 and USB connections, also functioning as a "data logger". The system employed was the Compact Field Point of National Instruments, model CFP 2000, with one module for acquisition of temperature through resistance, two modules for temperature acquisition through thermocouples, and one module for acquisition with current, as can be observed in Figures 5. The software LabView 8.0 was utilized in the construction of the control and acquisition computer code, including the data statistical treatment and the uncertainty analysis of the incorporated measurements.

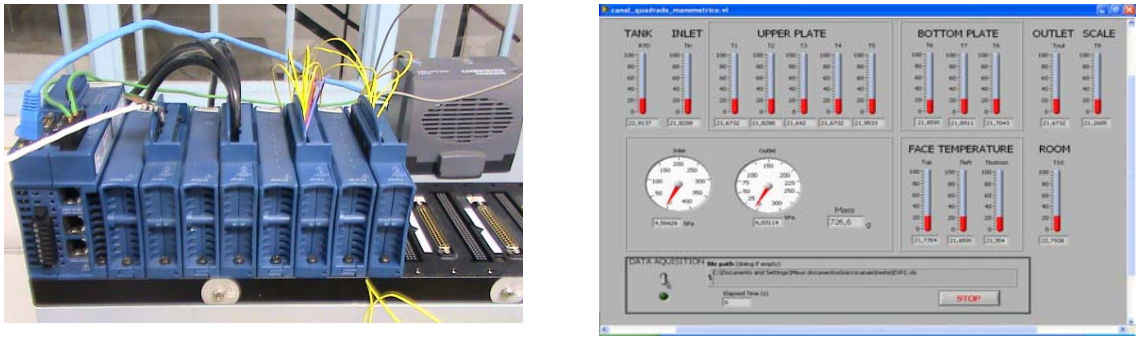

Figure 5: a) CFP2000 acquisition system with the acquisition and signal processing modules, b) screen of the software constructed with LabView 8.0 for control and acquisition.

An additional computational code was developed on the Mathematica 7.0 system for determining the propagation of uncertainties up to the evaluation of the local and mean Nusselt numbers, based on the temperature, mass flow rate, channel dimensions, and power generation measurements.

4. RESULTS AND DISCUSSION

The first step in the demonstration of the present implementation of the conjugated heat transfer problem in microchannels was to compare the obtained results with published ones for the symmetric case (Guedes et al. 1989, Elmor et al. 2005), also obtained through GITT but not accounting for heat generation within the walls and the fluid and for axial heat conduction along the fluid. Figure 6 thus presents the comparison of wall temperatures and local Nusselt numbers along the channel length, for the situation of symmetric boundary conditions with $Cj=10^{-4}$ and $Bi=1$ at both walls, but obtained with more general asymmetric model and code. Clearly, in both sets of results, the present implementation reproduces more closely the recent implementation in Elmor et al. (2005), which adopts an improved lumped-differential formulation for representing the average wall temperatures. One may also observe the expected reduction on the local Nusselt numbers as the longitudinal heat conduction plays some role in the heat transfer process,

especially towards the channel inlet region. It should be recalled that the present implementation accounts for the axial fluid conduction and truncation orders of up to N=30 were employed here.

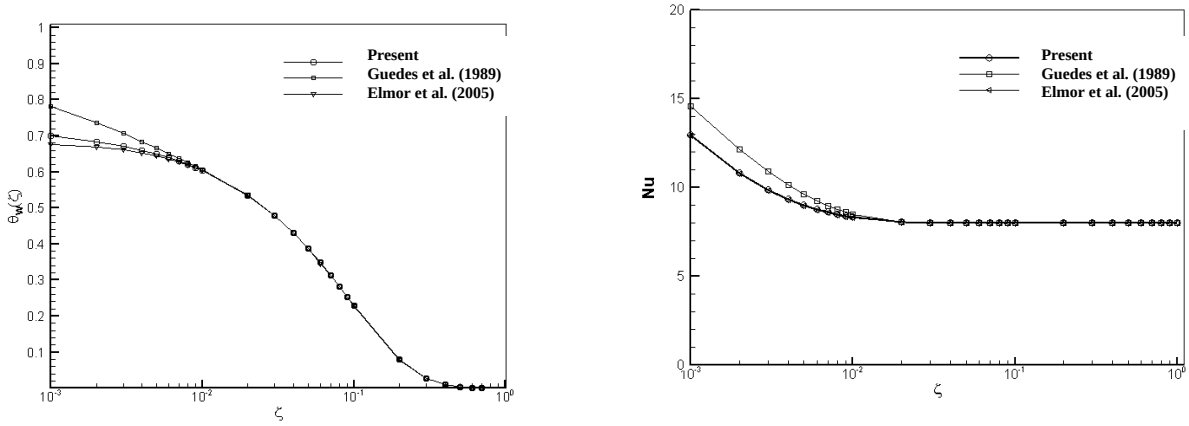

Figures 6. Comparison of present model for conjugated heat transfer in microchannels with previous solutions via GITT for the symmetric case with $Cj=10^{-4}$ and $Bi=1$ at both walls (Guedes et al. 1989, Elmor et al. 2005): a) Dimensionless wall temperature distribution; b)Local Nusselt number distributions.

Next, the proposed asymmetric model was verified through experimental measurements on the parallel plates micro-channel micro-machined from metallic plates of copper and tin, with adjustable spacing. The lower plate is heated by Joule effect and the whole set was encapsulated in the acrylic casing, being cooled by distilled water. Temperature measurements were then taken within both plates, and compared with the simulation results for the average wall temperatures. The range of Reynolds number analyzed was from Re=10 to 242. Sample graphs of such comparisons are shown in Figure 7 below, for a parallel plates spacing of 270 microns, and Re=13, 64, 122, and 224. The curves to the left refer to the measurements at the heated bottom wall, while the curves to the right are temperatures measured at the top wall. One may observe the marked influence of the Reynolds number on the heat transfer behavior, with some loss of adherence of the theoretical results for lower values of Re. Also, the model here proposed does not account for heat losses at the walls ends and for axial heat flow towards the entry tubing of the channel, beyond the heat transfer section, which start playing some role for such lower values of Peclet number and reducing the temperature gradients along the walls.

Table 1 brings a comparison of theoretical and experimental local Nusselt numbers at the middle of the channel length (x=L/2) and at the end (x=L), together with the corresponding values of Reynolds number, Prandtl number, and conjugation paramenters at the bottom and top walls. It can be seen that the conjugation parameters grow from around 10^{-4} for the higher values of Re, to almost 1 at the lower value of Re around 10. The model seems to account reasonably well for the governing physical effects, predicting the Nusselt numbers at both axial positions to within a maximum deviation of 3% in the range of parameters that has been investigated, with a slightly higher deviation for decreasing Reynolds number. The maximum uncertainty estimated for the Nusselt number experimental results was around 11%.

The experimental results for the local Nusselt numbers may also be examined over Figure 8 below, where the results are encapsulated by the theoretical values of the limiting situations of prescribed wall temperatures and prescribed wall heat fluxes. It can be noticed that for lower values of Re, when the conjugation parameters also markedly grow (see Table 1), the obtained Nusselt numbers approach the limiting solution of a prescribed uniform wall temperature, due to the longitudinal wall heat conduction effect. As the Reynolds number increases, the Nusselt number starts migrating towards the prescribed wall heat flux condition, with the progressive reduction of the conjugation effects. It should also be observed that for the higher values of Re, the Nusselt number values at x=L/2 and x=L deviate significantly, since at the middle of the channel (and eventually even at the end) one has not yet reached a fully developed condition, such as for the lower values of Re where they practically coincide.

In conclusion, the influence of conjugated convection-conduction heat transfer in microchannels was investigated, considering an asymmetric parallel-plates configuration, with heat generation in the walls, besides axial heat diffusion and viscous dissipation in the fluid. An experimental setup was built to measure the wall temperatures and evaluate Nusselt numbers along a tin-copper microchannel with 270 microns spacing between the parallel plates, heated at the bottom tin plate. In the range of parameters analyzed ($10<Re<250$), the relevance of wall conjugation was verified, and the simulated results provided an agreement within 3% against the experimental local Nusselt numbers along the channel. Conjugation deviates the thermal boundary condition from the expected simplified model of applied uniform heat flux, and at limiting situations brings the system behavior to that of a prescribed uniform temperature case. Thus, the simplified uniform wall heat flux modeling can induce an erroneous interpretation of heat transfer augmentation once conjugation effects are not accounted for in the interpretation of experimental results.

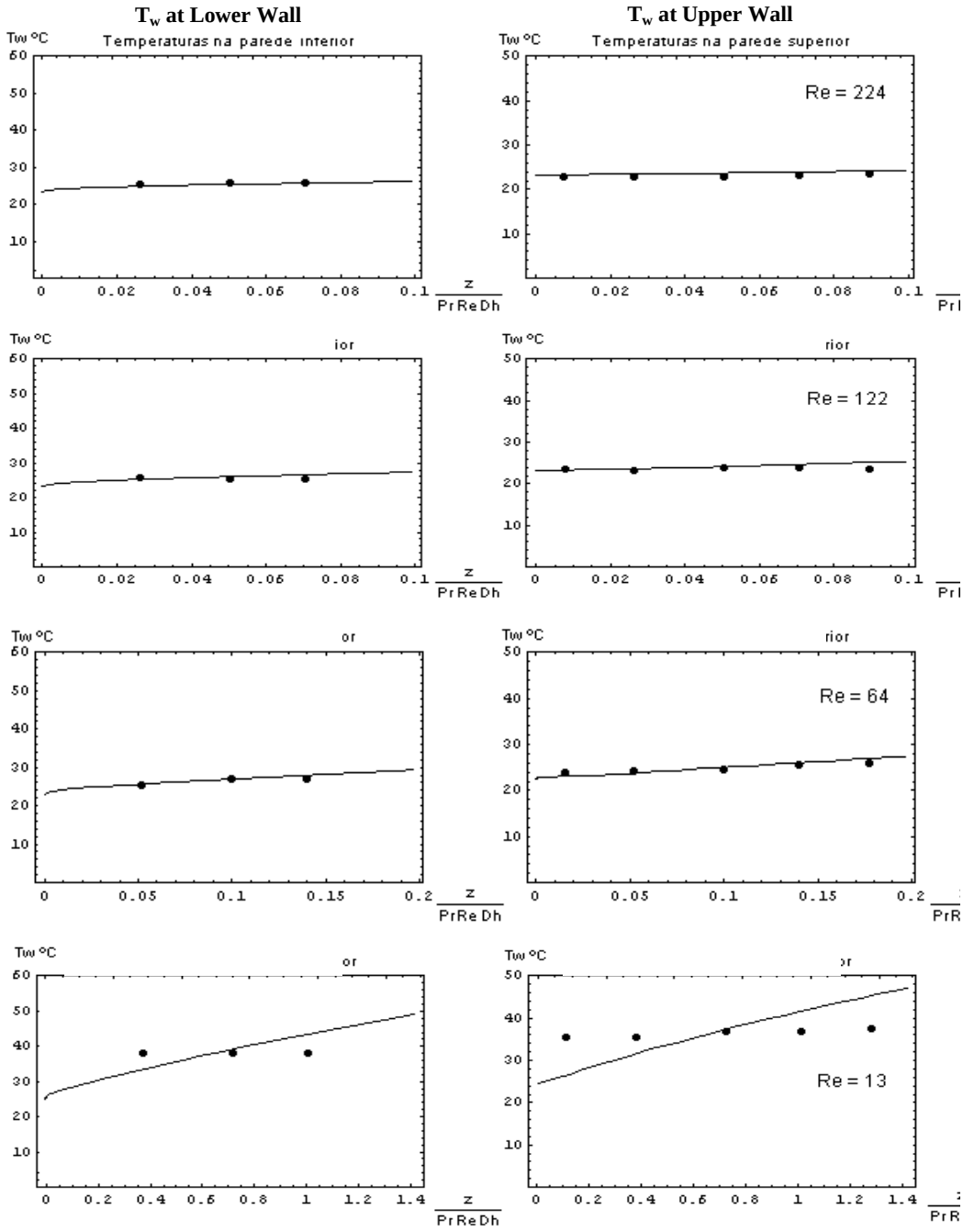

Figure 7. Comparison of measured (dots) and calculated (solid lines) wall temperatures for Re=224, 122, 64 and 13. (bottom heated plate– left, top plate – right).

Table 1 - Comparison of Simulation and Experiments for Local Nusselt Numbers in Microchannel (x=L/2 and x=L).

Run	Re	Pr	Cj1	Cj2	$Nu_{teo}(L/2)$	$Nu_{exp}(L/2)$	$Nu_{teo}(L)$	$Nu_{exp}(L)$
30_31	242.2	6.48	$2.86x10^{-4}$	$1.17x10^{-3}$	5.072	5.068	4.683	4.715
35_32	206.1	6.27	$4.26x10^{-4}$	$1.74x10^{-3}$	4.926	4.987	4.628	4.672
33_01	151.2	6.25	$7.86x10^{-4}$	$3.21x10^{-3}$	4.755	4.823	4.581	4.587
34_01	122.2	6.33	$1.18x10^{-3}$	$4.80x10^{-3}$	4.675	4.738	4.566	4.545
40_23	102.4	5.94	$1.89x10^{-3}$	$7.71x10^{-3}$	4.615	4.656	4.561	4.503
45_34	79.47	5.76	0.00332	0.0136	4.576	4.580	4.556	4.466
30_11	65.34	6.18	0.00429	0.0175	4.569	4.553	4.555	4.453
40_13	47.45	5.33	0.00947	0.0386	4.554	4.485	4.547	4.485
40_03	15.44	5.52	0.0954	0.389	4.509	4.380	4.488	4.499
50_05	10.82	5.01	0.234	0.955	4.473	4.385	4.440	4.374

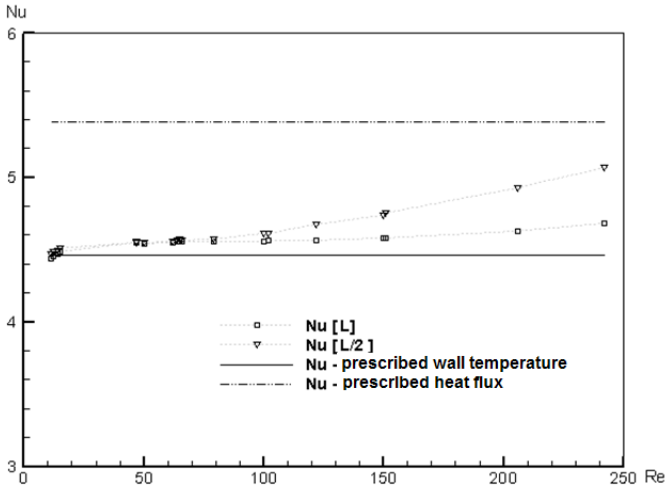

Figure 8. Comparison of measured (dots) local Nusselt numbers for parallel-plates microchannel against limiting fully developed values for prescribed wall temperature (solid line) and heat flux (dashed line). (Re ranging from 10 to 242).

5. ACKNOWLEDGEMENTS

The authors would like to acknowledge the financial support provided by CNPq, Brasil, RJ.

6. REFERENCES

Castellões, F.V., Cotta, R.M., 2006, Analysis of Transient and Periodic Convection in Micro-channels via Integral Transforms, Progress in Computational Fluid Dynamics, Vol. 6, 321-326.

Castellões, F.V., Cardoso, C.R., Couto, P., Cotta, R.M., 2007, Transient Analysis of Slip Flow and Heat Transfer in Microchannels, Heat Transfer Engineering, Vol.28, 549-558.

Castellões, F.V. and Cotta, R.M., 2008, Heat Transfer Enhancement in Smooth and Corrugated Microchannels, Proc. of the 7th Minsk Int. Seminar on Heat Pipes, Heat Pumps, Refrigerators, Invited Lecture, Minsk, Belarus, 8-11 September.

Castilho, A.M., 2003, Transferência de Calor em Microcanais, Dissertação de Mestrado, Instituto Militar de Engenharia, Rio de Janeiro.

Churchill, S.W., Ozoe, H., 1973, Correlations for Laminar Forced Convection in Flow over an Isothermal Flat Plate and in Developing and Fully Developed Flow in an Isothermal Tube", ASME J. Heat Transfer, Vol. 95 pp.416-23.

Cotta, R.M. [1993], Integral Transforms in Computational Heat and Fluid Flow, CRC Press, USA.

Cotta, R.M. and Gerk, J.E.V., 1994, Mixed Finite-difference/integral transform Approach for Parabolic-hyperbolic Problems in Transient Forced Convection, Numerical Heat Transfer, Part B, Vol. 25, 433-448.

Cotta, R.M., 1998, The Integral Transform Method in Thermal and Fluids Sciences and Engineering, Begell House, New York.

Cotta, R.M., Kakaç, S., Mikhailov, M.D., Castellões, F.V., Cardoso, C.R., 2005, Transient Flow and Thermal Analysis in Microfluidics, in: S. Kakaç, L.L. Vasiliev, Y. Bayazitoglu, Y. Yener. (Eds.), Microscale Heat Transfer – Fundamentals and Applications, NATO ASI Series, Kulwer Academic Publishers, Netherlands, 2005, pp. 175-196.

Cotta, R.M., Mikhailov, M.D., 2006, Hybrid Methods and Symbolic Computations, in: W.J. Minkowycz, E.M. Sparrow, and J.Y. Murthy (Eds.), Handbook of Numerical Heat Transfer, second ed., Wiley, New York, pp. 493-522.

Elmor, F.G., Guedes, R.O.C., and Scofano, F.N., 2005, Improved Lumped Solution for Conjugate Heat Transfer In Channel Flow with Convective Boundary Condition, Int. J. Heat & Technology, pp.78-88.

Guedes, R.O.C., Cotta, R.M. and Brum, N.C.L., 1989, Conjugated Heat Transfer in Laminar Flow Between Parallel - Plates Channel, 10th Brasilian Congress of Mechanical Engineering, Rio de Janeiro, Brasil.

Guedes, R.O.C., Cotta, R.M., and Brum, N.C.L., 1991, Heat Transfer in Laminar Tube Flow with Wall Axial Conduction Effects, J. Thermophysics & Heat Transfer, Vol. 5, no. 4, pp. 508-513.

Guedes, R.O.C. and Cotta, R.M., 1991, Periodic Laminar Forced Convection within Ducts Including Wall Heat Conduction Effects, Int. J. Eng. Sci, Vol. 29, n.5, pp. 535-547.

Luikov, A.V., Aleksashenko, V.A., and Aleksashenko, A.A., 1971, Analytical Methods of Solution of Conjugated Problems in Convective Heat Transfer, Int. J. Heat and Mass Transfer, Vol. 14, pp. 1047-1056.

Maranzana, G., Perry, I. e Maillet, D., 2004, Mini- and Micro-channels: Influence of Axial Conduction in the Walls, Int. J. Heat and Mass Transfer, Vol.47, pp. 3993-4004.

Mikhailov, M.D., and Cotta, R.M., 2005, Mixed Symbolic-Numerical Computation of Convective Heat Transfer with Slip Flow in Microchannels, Int. Comm. Heat & Mass Transfer, Vol. 32, Issues 3-4 , pp. 341-348.

Morini, G.L., 2004, Single-Phase Convective Heat Transfer in Microchannels: a Review of Experimental Results, Int. J. of Thermal Sciences, Vol.43, pp. 631-651.

Nunes, J.S., Couto, P., and Cotta, R.M., 2008, Conjugated Heat Transfer Problem in Rectangular Micro-channels under Asymmetric Conditions, Proc. of 5th National Congress of Mechanical Engineering, CONEM 2008, ABCM, Paper no. CON08-0739, Salvador, BA, August 2008.

Perelman, Y.L., 1961, On Conjugate Problems of Heat Transfer, Int. J. Heat and Mass Transfer, Vol. 3, pp.293-303.

Shah, R. K., 1975, Thermal Entry Solutions for the Circular Tube and Parallel Plates, Proc. of the 3rd National Heat and Mass Transfer Conf., Vol.1, Indian Institute of Technology, paper no. HMT-11-75, Bombay, India.

Sobhan, C.B. and Peterson, G.P., 2008, Microscale and Nanoscale Heat Transfer: Fundamentals and Engineering Applications, CRC Press, Boca Raton, FL.

Wolfram, S., 2008, The Mathematica Book, version 7.0, Cambridge-Wolfram Media.

Yener, Y., S. Kakaç, M. Avelino, T. Okutucu, 2005, Single-phase Forced Convection in Micro-channels – a State-of-the-art Review, in: S. Kakaç, L.L. Vasiliev, Y. Bayazitoglu, Y. Yener. (Eds.), Microscale Heat Transfer – Fundamentals and Applications, NATO ASI Series, Kluwer Academic Publishers, Netherlands, pp.1-24.

8. RESPONSIBILITY NOTICE

The authors are the only responsible for the printed material included in this paper.